The AAPS Journal, Vol. 16, No. 4, July 2014 (© 2014)
DOI: 10.1208/s12248-014-9613-8

Research Article

Theme: Natural Products Drug Discovery in Cancer Prevention
Guest Editors: Ah-Ng Tony Kong and Chi Chen

Apigenin Reactivates Nrf2 Anti-oxidative Stress Signaling in Mouse Skin Epidermal JB6 P+Cells Through Epigenetics Modifications

Ximena Paredes-Gonzalez,[1] Francisco Fuentes,[1] Zheng-Yuan Su,[1] and Ah-Ng Tony Kong[1,2]

Received 7 March 2014; accepted 25 April 2014; published online 16 May 2014

Abstract. Nrf2 is a crucial transcription factor that controls a critical anti-oxidative stress defense system and is implicated in skin homeostasis. Apigenin (API), a potent cancer chemopreventive agent, protects against skin carcinogenesis and elicits multiple molecular signaling pathways. However, the potential epigenetic effect of API in skin cancer chemoprotection is not known. In this study, bisulfite genomic DNA sequencing and methylated DNA immunoprecipitation were utilized to investigate the demethylation effect of API at 15 CpG sites in the Nrf2 promoter in mouse skin epidermal JB6 P+ cells. In addition, qPCR and Western blot analyses were performed to evaluate the mRNA and protein expression of Nrf2 and the Nrf2 ARE downstream gene, NQO1. Finally, the protein expression levels of DNA methyltransferases (DNMTs) and histone deacetylases (HDACs) were evaluated using API and the DNMT/HDAC inhibitor 5-aza/ trichostatin A. Our results showed that API effectively reversed the hypermethylated status of the 15 CpG sites in the Nrf2 promoter in a dose-dependent manner. API enhanced the nuclear translocation of Nrf2 and increased the mRNA and protein expression of Nrf2 and the Nrf2 downstream target gene, NQO1. Furthermore, API reduced the expression of the DNMT1, DNMT3a, and DNMT3b epigenetic proteins as well as the expression of some HDACs (1–8). Taken together, our results showed that API can restore the silenced status of Nrf2 in skin epidermal JB6 P+ cells by CpG demethylation coupled with attenuated DNMT and HDAC activity. These results may provide new therapeutic insights into the prevention of skin cancer by dietary phytochemicals.

KEY WORDS: apigenin; DNMTs; epigenetics; HDACs; JB6 P+; Nrf2; skin cancer.

INTRODUCTION

Skin cancers are the most common types of cancer in the US and worldwide (1,2). It is estimated that 81,220 men and women will be diagnosed with the disease in 2014 and that 12,980 will die (3). Ultraviolet radiation (UVR) between 200 and 400 nm is the most important risk factor leading to DNA damage, inflammation, immune impairment, and epigenetic modifications (4–6). Accumulating evidence shows that epigenetic silencing of critical tumor suppressor genes plays a role in cancer development and that enhanced DNA methylation at the C5 cytosine position of the CpG dinucleotides in the CpG island is associated with a transformed phenotype (7). In epidermis that is chronically exposed to UVR, there is a strong correlation among DNA methylation, augmented activity of DNA methyltransferases (DNMTs), and histone modifications (7). Thus, DNA methylation represents an early molecular event that precedes the observation of actual neoplastic lesions on the epidermis (8). In this context, diverse studies have revealed aberrant promoter methylation of many genes involved in critical cellular processes, including CDH1, CDH3, LAMA3, LAMC2, RASSF1A, BCL7a, PTPRG, thrombospondin 4, p73, p16, CHFR, p15, and TMS1 (6,8–10).

The deregulation of the antioxidant defense system has been gaining increased attention because it promotes toxicity and the neoplastic progression of cancer (11–13). In this context, we have reported that erythroid 2p45 (NF-E2)-related factor 2 (Nrf2), a basic region leucine zipper (bZIP) transcription factor that regulates the expression of many phase II detoxifying/antioxidant enzymes, is suppressed epigenetically by promoter CpG methylation/histone modifications in association with MBD2 in prostate tumors from TRAMP mice and tumorigenic TRAMP C1 cells (14). In addition, we have recently demonstrated that Nrf2 is down-regulated in 12-*O*-tetradecanoylphorbol-13-acetate (TPA)-induced neoplastic transformation of mouse skin epidermal JB6 P+cells (12). Thus, the reversible nature of epigenetic modifications is an attractive strategy to correct abnormal skin DNA methylation patterns using DNMT inhibitors, such as 5-azadeoxycytidine (5-aza) and 5-aza′-2-deoxycytidine (decitabine), or histone deacetylase (HDAC) inhibitors, such as romidepsin, trichostatin A (TSA), or vorinostat. However, the therapeutic use of these agents has been limited because

[1] Department of Pharmaceutics, Ernest Mario School of Pharmacy, Rutgers, The State University of New Jersey, 160 Frelinghuysen Road, Piscataway, New Jersey 08854, USA.
[2] To whom correspondence should be addressed. (e-mail: KongT@pharmacy.rutgers.edu)

of unacceptable toxic effects and the lack of gene modulation specificity (15). Thus, phytochemicals with minor side effects that have DNA methylation modulating properties are a promising alternative for skin cancer chemoprevention (16).

Apigenin (API) is the most important and active flavonoid present in chamomile flowers (*Matricaria recutita* L.), a common component of many skin formulations used in folk medicine since the time of Hippocrates in 500 BC (17). API has long been recognized to be active against skin carcinogenesis, exerting a broad spectrum of activities, including DNA damage prevention, cell cycle arrest, and apoptosis induction, as well as immunomodulatory and anti-inflammatory effects with high tumor specificity activity, low toxicity, and the ability to penetrate deep skin layers in mice and humans (18–22). Thus, topical application of API potently suppresses epidermal ornithine decarboxylase activity, which directly promotes skin carcinogenesis by enhancing cell proliferation, angiogenesis, and metastasis in susceptible mouse strains after administration of TPA or UV irradiation (23,24). Moreover, API treatment of SENCAR mice reduces papilloma incidence induced by TPA/7,12-dimethylbenz(a)anthracene (DMBA) by more than 50%, thereby reducing the conversion from papilloma to carcinoma and increasing the latency period for tumor conversion (23). Similarly, a reduction in tumorigenesis has been observed after topical application of API in SKH-1 mice exposed to chronic UV irradiation (24) and in intraperitoneal administration in syngeneic C57BL6 mice injected with B16–BL6 cells (25). Interestingly, API induces epigenetic modifications due to its capacity to produce 5-methylcytosine inhibition in the human KYSE-510 esophageal squamous cell carcinoma cell line (26) and HDAC inhibition in PC3 and 22Rv1 prostate cancer cell lines (27). In this study, we investigated the potential of API to restore the expression of Nrf2 through DNA methylation in the preneoplastic epidermal JB6 P+cell line.

MATERIALS AND METHODS

Reagents

All chemicals, including API, dimethyl sulfoxide (DMSO), 5-aza-2′-deoxycytidine (5-aza), and TSA, were purchased from Sigma (St. Louis, MO). The murine skin epidermal JB6 P+cell line, Cl 41-5a, was purchased from American Type Culture Collection (ATCC, Rockville, MD). JB6 P+cells were maintained in minimum essential media (MEM) supplemented with 5% (*V/V*) fetal bovine serum (FBS; GiBco, Invitrogen Corp., USA), 100 U/ml penicillin and 100 μg/ml streptomycin. Cells were maintained in a humidified incubator with 5% CO_2 at 37°C.

MTS Assay

JB6 P+cells were cultured in 96-well plates using MEM containing 5% FBS at densities of 2×10^5 cells/ml for the 1- and 3-day treatments and 5×10^4 cells/ml for the 5-day treatment. After 24 h, the cells were treated with MEM/1% FBS and various concentrations of API using 0.1% DMSO as a control. For the 3- and 5-day treatments, the medium containing drugs was changed every 2 days. The cytotoxicity of API was tested using the CellTiter 96 aqueous non-radioactive cell proliferation MTS assay [3-(4,5-dimethylthiazol-2-yl)-5-(3-carboxymethoxyphenyl)-2-(4-sulfophenyl)-2H-tetrazolium, inner salt; MTS] (Promega, Madison, WI). After the 1-, 3-, and 5-day treatments, the JB6 P+cells were treated with the MTS solution for 1 h at 37°C. Absorbance of the formazan product was read at 490 nm using a μQuant Biomolecular Spectrophotometer (Bio-Tek Instruments Inc., Winooski, VT), and cell viability was calculated in comparison with the control DMSO.

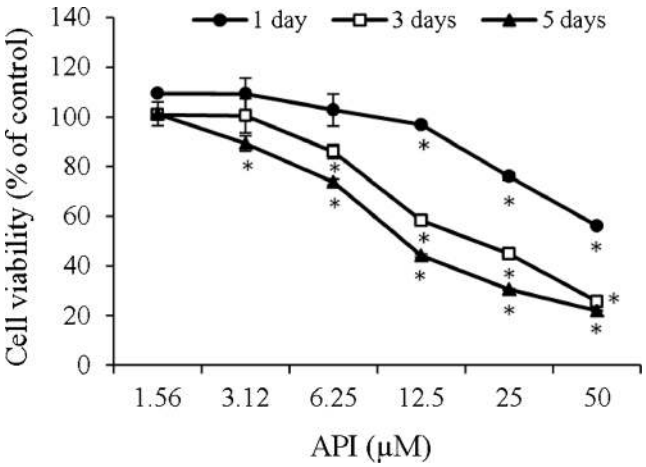

Fig. 1. API exhibits cytotoxicity against JB6 P+cells. Cells were seeded in 96-well plates in 5% MEM for 24 h. The cells were then incubated in fresh medium with API for 1, 3, or 5 days at different concentrations (1.56 to 50 μM), as described in the "Materials and Methods." Cell viability was determined and calculated using the MTS assay. The data are expressed as the mean±SD (n=3). *Asterisk* indicates significant differences ($p<0.05$) in cell viability in comparison with the control

RNA Extraction and Quantitative Real-Time PCR

JB6 P+cells were cultured in 10-cm plates using MEM containing 1% FBS at a density of 5×10^3 cells/ml. After 24 h, the cells were treated with 1.56 or 6.25 μM API for 5 days using 0.1% DMSO and 100 nM 5-aza as negative and positive controls, respectively. The medium containing drugs was changed every 2 days. For the 5-aza/TSA treatment, 100 nM TSA was added to the 5-aza-containing medium on day 4, and the cells were cultured for an additional 24 h. The cells were then harvested for RNA isolation. Total RNA was extracted using the RNeasy Mini Kit (QIAGEN, Valencia, CA). First-strand cDNA was synthesized from 1 μg of total RNA using the SuperScript III First-Strand Synthesis System for RT-PCR (Invitrogen, Carlsbad, CA) according to the manufacturer's instructions. The cDNA was used as the template for quantitative real-time PCR (qPCR) with Power SYBR Green PCR Master Mix (Applied Biosystems, Carlsbad, CA) in an ABI7900HT system. The following sequences for the Nrf2 and NQO1 primers were used: Nrf2, 5′-GGCAGAGACATTCCCATTTGTAG-3′ (sense) and 5′-TCGCCAAAATCTGTGTTTAAGGT-3′ (antisense); and NQO1, 5′-CAGAAATGACATCACAGGTGAGC-3′ (sense) and 5′-CTAAGACCTGGAAGCCACAGAAA-3′ (antisense). β-Actin was used as an internal control with

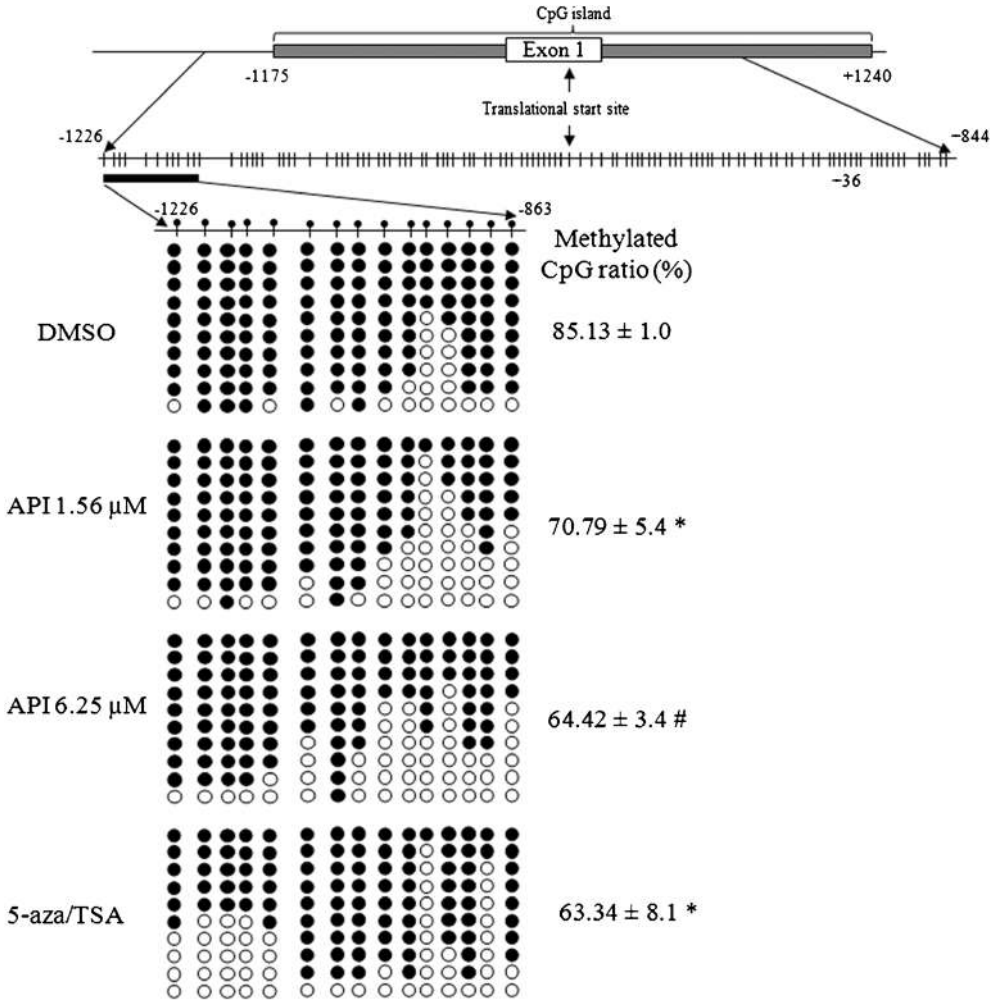

Fig. 2. API decreases the methylation level of 15 CpG sites in the Nrf2 promoter in JB6 P+cells. The methylation level at the 15 CpG sites in the Nrf2 promoter was determined using bisulfite genomic sequencing (BGS), as described in the "Materials and Methods." The 15 CpGs sites were located between -1226 and -863 of the murine Nrf2 gene with the translational start site defined as +1. The cells were seeded and treated for 5 days with 1.56 and 6.25 μM API as well as the combination of 5-aza/TSA. *Black dots* indicate methylated CpGs, and *open circles* indicate non-methylated CpGs. The values are the mean±SD of at least ten clones from three independent experiments. *Asterisk* and *number sign* indicate significant differences ($p<0.05$ and $p<0.01$, respectively) in methylation level in comparison with control DMSO

sense (5′-CGTTCAATACCCCAGCCATG-3′) and antisense (5′-GACCCCGTCACCAGAGTCC-3′) primers.

Protein Lysate Preparation and Western Blotting

JB6 P+cells were treated using the procedures described above. After the 5 days of treatment, cells were harvested using RIPA buffer supplemented with a protease inhibitor cocktail (Sigma, St. Louis, MO) to obtain whole protein lysate. In the case of nuclear protein extraction, the NEPER Nuclear and Cytoplasmic Protein Extraction Kit (Pierce, Rockford, IL) was used according to the manufacturer's instructions. The protein concentrations of the cleared lysates were determined using the bicinchoninic acid method (Pierce, Rockford, IL), and 20 μg of total protein from each sample was mixed with 5 μl of Laemmli's sodium dodecyl sulfate (SDS)-sample buffer (Boston Bioproducts, Ashland, MA, USA) and denatured at 95°C for 5 min. The proteins were separated using 4–15% SDS-polyacrylamide gel electrophoresis (Bio-Rad, Hercules, CA) and were then transferred to a polyvinylidene difluoride membrane (Millipore, Bedford, MA) followed by blocking with 5% BSA in Tris-buffered saline-0.1% Tween 20 buffer. The membrane was then sequentially incubated with specific primary antibodies and HRP-conjugated secondary antibodies. The blots were visualized by the SuperSignal enhanced chemiluminescence detection system and recorded using a Gel Documentation 2000 system (Bio-Rad, Hercules, CA). The primary antibodies were purchased from different sources as follows: anti-Nrf2, anti-NQO1, anti-β-actin, and anti-Lamin A antibodies were purchased from Santa Cruz Biotechnology (Santa Cruz, CA); anti-DNMT1, anti-DNMT3a, and anti-DNMT3b antibodies were purchased from IMGENEX (San Diego, CA); anti-HDAC1 to anti-HDAC6 antibodies were purchased from Cell Signaling (Boston, MA); anti-HDAC7 antibody was purchased from Millipore (Bedford, MA); and anti-HDAC8 antibody was purchased from Proteintech (Chicago, IL).

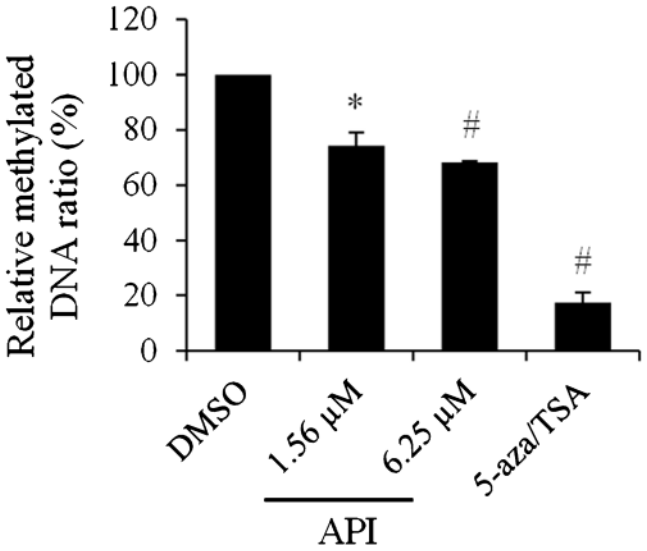

Fig. 3. API significantly decreases the binding of anti-methyl cytosine antibody to the 15 CpGs sites in the Nrf2 promoter in JB6 P+cells. Methylated DNA immunoprecipitation (MeDIP) was performed as described in the "Materials and Methods" using the MagMEDIP kit. The immunoprecipitated DNA and inputs were analyzed by qPCR using primers covering the 15 CpG sites in the Nrf2 promoter. The relative amount of MeDIP DNA was calculated using a standard curve of delta CT values obtained by serial dilution of the inputs. The relative values were then compared with the DMSO control, which was defined as 100% of methylated DNA. The values are expressed as the mean±SD of three separate samples. *Asterisk* and *number sign* indicate significant differences ($p<0.05$ and $p<0.01$, respectively) in the relative methylated DNA ratio in comparison with control DMSO

Bisulfite Genomic Sequencing (BGS)

Genomic DNA was isolated from DMSO-, API-, or 5-aza/TSA-treated JB6 P+cells using the QIAamp® DNA Mini Kit (Qiagen, Valencia, CA). The bisulfite conversion was performed using 500 ng of genomic DNA with the EZ DNA Methylation Gold Kit (Zymo Research Corp., Orange, CA) following the manufacturer's instructions. The converted DNA was amplified by PCR using Platinum Taq DNA polymerase (Invitrogen, Grand Island, NY) and primers that amplify the 15 CpG sites located between -1226 and -863 of the murine Nrf2 gene with the translational start site defined as +1. The sequences of the primers were as follows: 5′-AGTTATGAAGTAGTAGTAAAAA-3′ (sense) and 5′-AATATAATCTCATAAAACCCCAC-3′ (antisense) for the first five CpG sites; and 5′-TTAAAAATAGTTTGAGAGGTG-3′ (sense) and 5′-ACCCCAAAAAAATAAATAAATC-3′ (antisense) for the next ten CpG sites. The PCR products were cloned into the pCR4 TOPO vector using a TOPO™ TA Cloning Kit (Invitrogen, Carlsbad, CA). Plasmids from at least ten colonies of each treatment group were prepared using the QIAprep Spin Miniprep Kit (Qiagen, Valencia, CA) and were sequenced (Genwiz, Piscataway, NJ).

Methylated DNA Immunoprecipitation (MeDIP) Analysis

MeDIP analysis was performed with a MagMeDIP Kit (Diagenode, Denville, NJ) according to the manufacturer's instructions as described previously (14,28). Briefly, the extracted DNA from the treated JB6 P+cells was sonicated on ice to approximately 100–500 bp. The fragmented DNA was denatured at 95°C for 3 min and subjected to immunoprecipitation overnight at 4°C. After incubation, the DNA contained on the magnetic beads with an anti-methylcytosine antibody (Anaspec, Fremont, CA), and an anti-c-Myc antibody (as a negative control; Santa Cruz, Santa Cruz, CA) was isolated for use in PCR and qPCR assays. The primers, 5′-TTTCTAGTTGGAGGTCACCACA-3′ (sense) and 5′-CCCAGGGAGATGGATGAGT-3′ (antisense), were used to cover the DNA sequence of the 15 CpG sites of murine Nrf2 from position -1,226 to -863 with the translational start site defined as +1. The enriched MeDIP DNA content was calculated on the basis of the calibration of the serial dilution of input DNA by qPCR, and the relative methylated DNA ratios were calculated on the basis of the control, which was defined as 100% methylated DNA (29).

Statistical Analysis

All experiments were performed at least three times with similar results. Statistical tests were performed using Student's *t* test. All *p* values were two-sided, and a *p* value <0.05 was considered statistically significant.

RESULTS

API Exhibits Cytotoxicity Against JB6 P+Cells

The cell viability of JB6 P+cells was analyzed to determine the cytotoxic effect of API using a MTS assay. The results showed that API treatments decreased cell viability in a dose-dependent manner at 1, 3, and 5 days after treatment (Fig. 1). Low concentrations of API (<6.25 μM) were much less toxic than higher concentrations (50 μM). Because the viability of cells treated with 6.25 μM API was greater than 70%, API concentrations of 1.56 and 6.25 μM were selected for subsequent studies of epigenetic modifications of the Nrf2 gene promoter.

API Decreases the Methylation Level of 15 CpG Sites in the Nrf2 Promoter in JB6 P+Cells

We previously demonstrated that the transcriptional activity of Nrf2 is significantly downregulated when the first 15 CpG sites of the Nrf2 promoter are hypermethylated in JB6 P+cells (12). Therefore, we performed bisulfite genomic sequencing (BGS) to determine whether API treatment demethylated these CpG sites during a 5-day treatment with 0.1% DMSO and the combination of 5-aza/TSA (100/100 nM) as controls. We found that JB6 P+cells treated with DMSO were highly methylated (85%; Fig. 2), which was in agreement with our previous studies (12). Treatments with API significantly decreased ($p<0.05$) the methylation status of these CpG sites in a dose-dependent manner (Fig. 2). Similarly, the combination of the DNMT/HDAC inhibitors (5-aza/TSA) showed significant demethylation ($p<0.05$)

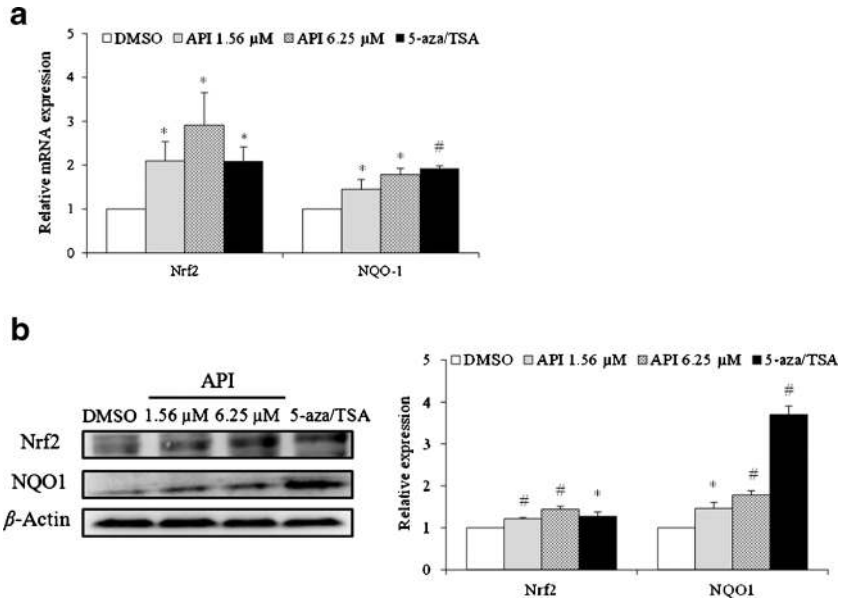

Fig. 4. API increases the level of mRNA and protein expression of Nrf2 and the Nrf2 downstream gene, NQO1. **a** Relative fold changes of mRNA expression of Nrf2 and NQO1 in JB6 P+cells treated with API, DMSO, and the DNMT/HDAC inhibitor (5-aza/TSA) combination. After 5 days of treatment, mRNA expression was determined using the ABI7900HT qPCR system. Normalization of gene expression data was performed using β-actin as an internal control. The data are expressed as the mean±SD of three independent experiments. The primer sequences are described in the "Materials and Methods." *Asterisk* and *number sign* indicate significant differences ($p<0.05$ and $p<0.01$, respectively) in relative mRNA expression level in comparison with control DMSO. **b** Protein expression level of Nrf2 and the downstream gen NQO1 in JB6 P+cells treated with DMSO, API, and the DNMT/HDAC inhibitor (5-aza/TSA) combination for 5 days. *Asterisk* and *number sign* indicate significant differences ($p<0.05$ and $p<0.01$, respectively) in relative protein expression in comparison with control DMSO. The images were analyzed using ImageJ software (NIH, http://rsbweb.nih.gov/ij/). The protein expression level was normalized with β-actin (a complete description of the procedure and antibodies used is presented in the "Materials and Methods")

compared with DMSO-treated cells (63%; Fig. 2). These results strongly suggested that API demethylated the Nrf2 promoter in a dose-dependent manner and acted preferentially on the last ten CpG sites analyzed (Fig. 2).

API Significantly Decreases the Binding of Anti-methyl Cytosine Antibody to the 15 CpG Sites in the Nrf2 Promoter in JB6 P+Cells

To confirm our findings, we performed a methylated DNA immunoprecipitation (MeDIP) assay in which methylated DNA fragments are enriched *via* immunoprecipitation with an anti-methylcytosine (anti-MeCyt) antibody that binds specifically to methylated cytosine. The enriched methylated DNA was used as the template for qPCR analysis to amplify the Nrf2 promoter region containing the CpG sites of interest (Fig. 3). The qPCR results showed that API and the 5-aza/TSA combination significantly reduced the total amount of MeCyt enrichment of the 15 CpG sites in the Nrf2 promoter compared to the control ($p<0.05$). Thus, these results strongly suggested that API can reverse the methylation level of these specific CpG sites in the Nrf2 promoter in JB6 P+ cells.

API Increases mRNA and Protein Expression Levels of Nrf2 and Nrf2 Downstream Genes

We have previously demonstrated that Nrf2 and Nrf2 downstream genes are decreased in JB6 P+cells (12). To evaluate whether the demethylation induced by API in the promoter region of Nrf2 contributed to the transcriptional activation of Nrf2 and Nrf2 downstream genes, we first examined the expression of Nrf2 and NQO1 by qPCR (Fig. 4a). The results revealed that the gene expression levels of Nrf2 and the ARE-mediated gene NQO1 were significantly ($p<0.05$) increased in API-treated JB6 P+cells in a dose-dependent manner compared with the control. Similarly, the gene expression levels of Nrf2 and NQO1 were also significantly ($p<0.05$) increased in the 5-aza/TSA treatment. We next assessed the protein levels of Nrf2 and NQO1 by Western blot analysis. Figure 4b shows that the protein levels of the Nrf2 and the Nrf2 downstream gene NQO1 were in agreement with the previous findings, especially at the higher dose of API for Nrf2. Interestingly, NQO1 protein expression was high in the 5-aza/TSA treatment. In order to confirm the effect of API in JB6 P+cells, we assessed the nuclear translocation of Nrf2 induced by API. After 5 days of treatment, API at 1.56 and 6.25 μM significantly

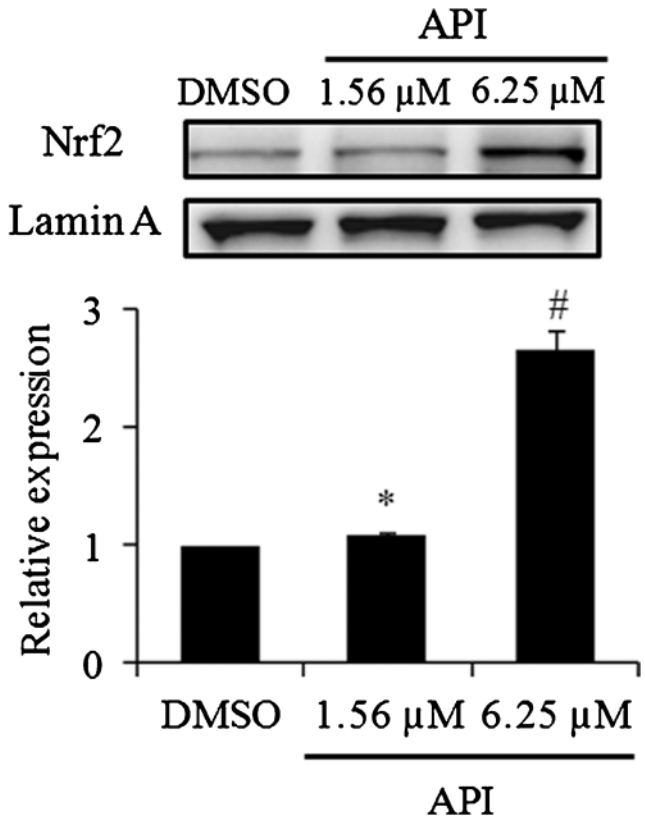

Fig. 5. API increases the level of the nuclear translocation of the Nrf2 protein. JB6 P+cells were treated with DMSO and API for 5 days. *Asterisk* and *number sign* indicate significant differences ($p<0.05$ and $p<0.01$, respectively) in relative protein expression in comparison with control DMSO. The images were analyzed by ImageJ software (NIH, http://rsbweb.nih.gov/ij/). The protein expression level was normalized with Lamin A (a complete description of the procedure and antibodies used is presented in the "Materials and Methods")

increased the nuclear translocation of the Nrf2 protein in JB6 P+cells compared with the control group (Fig. 5). These results suggest that API has the potential to increase the Nrf2-mediated mRNA and protein expression of Nrf2 downstream genes, which might be correlated with the increased cellular expression and nuclear translocation of Nrf2 in JB6 P+cells.

API Induces Modifications in the Expression of DNMT and HDAC Proteins

Because DNA methylation occurs at the 5′ position of the cytosine residue within CpG dinucleotides through the addition of a methyl group by DNA methyltransferases (DNMTs), including DNMT1, DNMT3A, and DNMT3B (11), we next evaluated the effect of API on DNMT protein expression. Figure 6a shows that API decreased the expression of all DNMTs, especially DNMT1 and DNMT3b, at the higher dose. Furthermore, the expression of all DNMTs was also decreased by the combination treatment of 5-aza/TSA as expected.

Previous studies have reported that API decreases HDAC class I activity, specifically HDAC1 and HDAC3 proteins, in prostate cancer cells with a concomitant global acetylation of histones H3 and H4 (27). To assess the effect of API on HDAC proteins in JB6 P+cells, we evaluated HDAC class I and class II proteins. We observed that API decreased the expression of HDACs (1–8) in a dose-dependent manner (Fig. 6b). Nevertheless, HDAC1 and HDAC5 proteins were slightly decreased at the higher dose of API, but the expression of HDAC3, HDAC4, HDAC6, and HDAC8 was affected by both doses. Interestingly, the combination of 5-aza/TSA dramatically decreased the protein expression of all HDAC proteins assessed, except for HDAC7, which was not affected compared with the control. Taken together, API decreased DNMT and HDAC expression in a dose-dependent manner, which was in general comparable with the 5-aza/TSA combination treatment at the higher dose.

DISCUSSION

The generation of reactive oxygen species (ROS) is an essential metabolic process for maintaining homeostasis in the human body, and it serves as an important sensor in skin (11,30). Thus, ROS at low levels initiate cell cycle arrest and promote DNA repair mechanisms, but ROS at high levels initiate apoptosis though activation of death receptor signaling (30). The imbalance between the generation of ROS and the anti-oxidative stress defense systems in the body can be highly deleterious to the cells because they need effective mechanisms for detoxification, such as the ARE gene machinery orchestrated by Nrf2, which contributes to the preservation of skin homeostasis (11,31). Previously, we have reported the critical role of Nrf2, a key transcription factor that regulates the expression of many phase II detoxifying/antioxidant enzymes, in the classical 2 stage carcinogenesis model with the DMBA chemical carcinogen and the tumor promoter TPA-induced skin cancer in Nrf2 KO mice (32). Thus, the transcriptional repression of Nrf2 and ARE target genes contributes to cell transformation allowing enhanced effects of carcinogens due to impaired functional protection (33,34). We have also demonstrated that Nrf2 expression is regulated by epigenetic mechanisms during tumor promoter TPA-induced mouse skin cell transformation, thereby suggesting the epigenetic reactivation of Nrf2 and the subsequent induction of Nrf2 downstream target genes involved in cellular protection (12).

In contrast, *in vitro* and *in vivo* studies have shown that API is an active compound against skin carcinogenesis (19) and targets many pathways as follows: G1 cell cycle arrest with the induction of p21/WAF1 (35) and G2/M cell cycle arrest inducing the inhibition of the p34 (cdk2) kinase

Fig. 6. API changes the expression of DNMT and HDAC proteins. **a** Protein expression level of DNMT1, DNMT3a, and DNMT3b. **b** Protein levels of the HDAC (1–8) enzymes. JB6 P+cells were treated with DMSO, API, or the DNMT/HDAC inhibitor (5-aza/TSA) combination for 5 days. *Asterisk* and *number sign* indicate significant differences ($p<0.05$ and $p<0.01$, respectively) in relative protein expression in comparison with control DMSO. The images were analyzed by ImageJ software (NIH, http://rsbweb.nih.gov/ij/). The protein expression level was normalized with β-actin (a complete description of the procedure and antibodies used is presented in the "Materials and Methods")

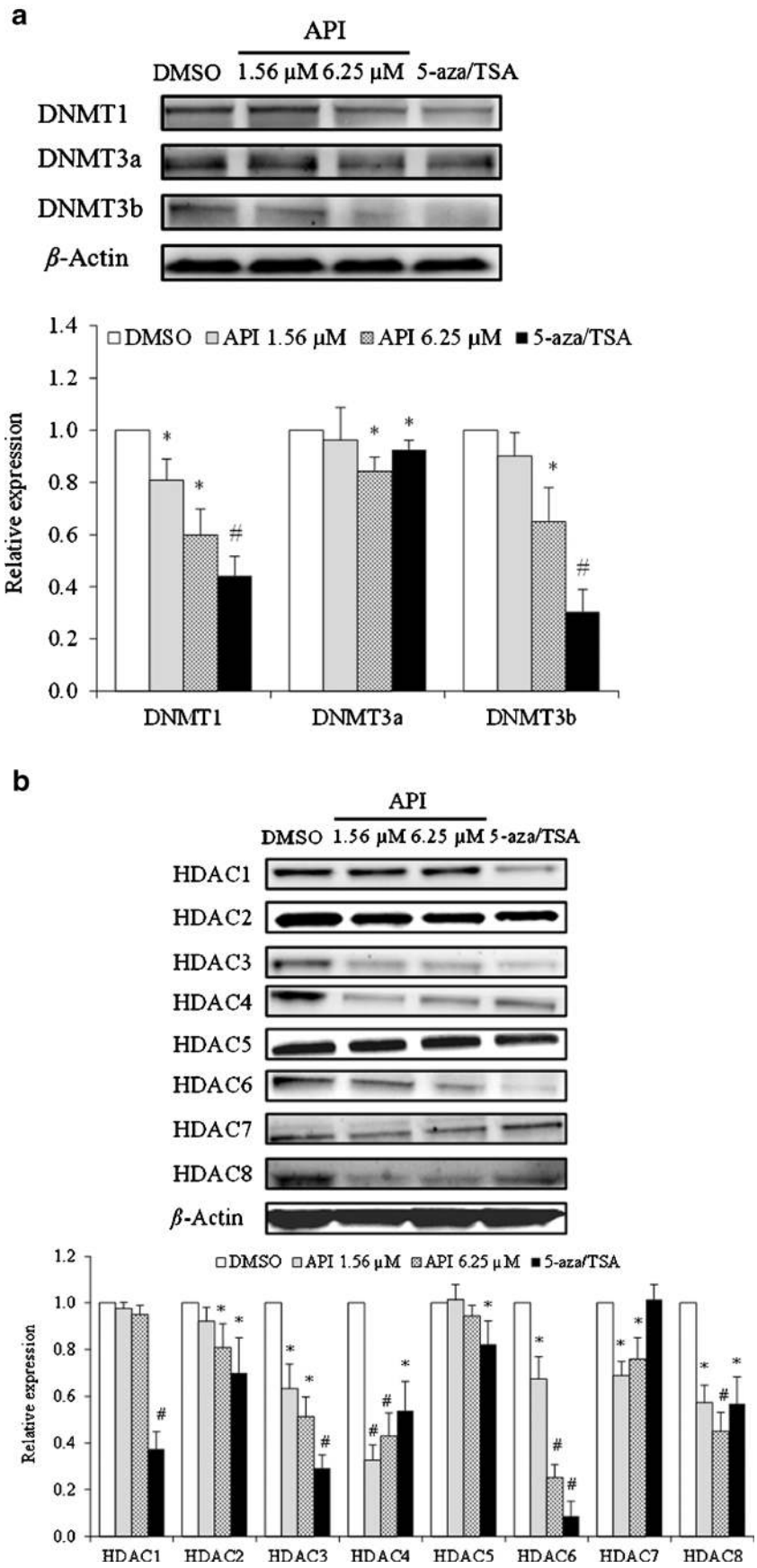
a
API
DMSO 1.56 μM 6.25 μM 5-aza/TSA
DNMT1
DNMT3a
DNMT3b
β-Actin
DMSO API 1.56 μM API 6.25 μM 5-aza/TSA
Relative expression
DNMT1
DNMT3a
DNMT3b
b
API
DMSO 1.56 μM 6.25 μM 5-aza/TSA
HDAC1
HDAC2
HDAC3
HDAC4
HDAC5
HDAC6
HDAC7
HDAC8
β-Actin
DMSO API 1.56 μM API 6.25 μM 5-aza/TSA
Relative expression
HDAC1
HDAC2
HDAC3
HDAC4
HDAC5
HDAC6
HDAC7
HDAC8

independent activation of p21/WAF1 (36), p53 stabilization, and p53 expression through the modulation of p53–HuR protein interaction (37), blockade of protein kinase C activity (38), inhibition of inducible cyclo-oxygenase-2 (COX-2) (39,40), and inhibition of Src kinase (41). Thus, more than 150 human cellular targets associated with API have been identified revealing the complex biological network targeted by this flavone (42). In addition, API induces epigenetic modifications that inhibit 5-cytosine DNA methyltransferase activity in human KYSE-510 esophageal squamous cell carcinoma cells and HDAC inhibition in PC3 and 22Rv1 prostate cancer cells (26,27,43). However, there are no data revealing the molecular mechanisms of API behind the epigenetic regulation of Nrf2 in mouse skin cells. In this study, we presented data demonstrating that API reversed the methylation status of 15 specific CpG sites in the promoter region of the Nrf2 gene in JB6 P+cells by BGS and MeDIP analyses (Figs. 2 and 3). Moreover, the results from this study also revealed that the expression of Nrf2 and Nrf2 downstream targets, namely NQO1, in JB6 P+cells was restored after treatment with API and the DNMT/HDAC inhibitors (5-aza/TSA) (Fig. 4) and that API was able to induce the nuclear translocation of Nrf2 in a dose-dependent manner (Fig. 5).

To elucidate the specific demethylation effects of API on the CpG sites in the Nrf2 promoter, we evaluated the protein expression of DNMT1, DNMT3a, and DNMT3b. The decreased DNMT expression, especially DNMT1 and DNMT3b (Fig. 6a), observed in the present study was in agreement with previous studies indicating that API has high affinity for GC-rich DNA in the GSTP-1 promoter sequence of prostate cancer cells, thus preventing the methylation of this promoter sequence when incubated with the MssI enzyme (44). Similarly, API has been reported to inhibit the 5-cytosine DNA methyltransferase activity in nuclear extracts of KYSE 510 cells (26). Nevertheless, the specific effect on the maintenance of DNMT1 and the *de novo* methyltransferases, namely DNMT3a and DNMT3b, has not been fully elucidated.

It has been observed that UVB-induced skin tumors in mice show elevated expression and activity of the DNMT1, DNMT3a, and DNMT3b with potential role in the suppression of the immune system and inflammatory response (6). Similarly, DNMT3a and DNMT3b have been reported highly expressed in human metastatic melanoma, and they are associated with poor prognosis (45). This suggests that API could potentially may play an important role in controlling the expression of DNMTs during UVB-induced skin cancer.

We also evaluated the effect of API on the expression of HDAC proteins in JB6 P+cells because API has been reported to inhibit HDAC1 and HDAC3 proteins in human prostate cancer cells, resulting in global histone H3 and H4 acetylation as well as localized hyperacetylation of histone H3 on the p21/waf1 promoter, leading to induction of growth arrest and apoptosis (27). Although studies of histone modifications are scarce in non-melanoma skin cancer, it has been reported that elevated expression of HDACs is associated with closed chromatin and transcriptional repression which may play an important role in DNA repair mechanisms after environmental insults such as ultraviolet radiation (6,46). Our results revealed that API is not only able to target HDAC class I proteins (HDAC1, HDAC2, HDAC3, HDAC8) but also class IIA (HDAC4, HDAC7) and class IIB (HDAC6) proteins, thereby inhibiting almost all HDACs evaluated (1–8), except for HDAC5, in a dose-dependent manner (Fig. 6b).

CONCLUSIONS

The results of this study demonstrated that API demethylates the Nrf2 gene promoter at 15 specific CpG sites in JB6 P+cells *in vitro* and that its activity is mediated though the inhibition of DNMT and HDAC proteins, which restore the cellular expression and nuclear translocation of Nrf2 and the Nrf2 downstream target, NQO1. These findings provide new insights into earlier observations that have shown differential Nrf2 expression during tumor promoter TPA-induced mouse skin cell transformation (12). In sum, the present study supports the conclusion that API may play an important role in the prevention and treatment of skin cancer by epigenetic modifications, leading to therapeutic development as a primary chemopreventive agent and/or as an adjuvant therapy.

ACKNOWLEDGMENTS

We thank all the members in Dr. Ah-Ng Tony Kong's lab for their helpful discussion and preparation of this manuscript. This work was supported by institutional funds.

Conflict of interest No potential conflicts of interest were disclosed.

REFERENCES

1. Lomas A, Leonardi-Bee J, Bath-Hextall F. A systematic review of worldwide incidence of nonmelanoma skin cancer. Br J Dermatol. 2012;166(5):1069–80.
2. Lewis KG, Weinstock MA. Trends in nonmelanoma skin cancer mortality rates in the United States, 1969 through 2000. J Invest Dermatol. 2007;127(10):2323–7.
3. Siegel R, Ma J, Zou Z, Jemal A. Cancer statistics, 2014. CA: A Cancer J Clin. 2014;64(1):9–29.
4. Halliday GM, Byrne SN, Damian DL. Ultraviolet A radiation: its role in immunosuppression and carcinogenesis. Semin Cutan Med Surg. 2011;30(4):214–21.
5. Hussein MR. Ultraviolet radiation and skin cancer: molecular mechanisms. J Cutan Pathol. 2005;32(3):191–205.
6. Nandakumar V, Vaid M, Tollefsbol TO, Katiyar SK. Aberrant DNA hypermethylation patterns lead to transcriptional silencing of tumor suppressor genes in UVB-exposed skin and UVB-induced skin tumors of mice. Carcinogenesis. 2011;32(4):597–604.
7. Jones PA, Baylin SB. The fundamental role of epigenetic events in cancer. Nat Rev Genet. 2002;3(6):415–28.
8. Sathyanarayana UG, Moore AY, Li L, Padar A, Majmudar K, Stastny V, *et al*. Sun exposure related methylation in malignant and non-malignant skin lesions. Cancer Lett. 2007;245(1–2):112–20.
9. Brown VL, Harwood CA, Crook T, Cronin JG, Kelsell DP, Proby CM. p16INK4a and p14ARF tumor suppressor genes are

commonly inactivated in cutaneous squamous cell carcinoma 2004 [cited 122 5]. 1284-92]. Available from: <Go to ISI>:// MEDLINE:15140233.
10. van Doorn R, Zoutman WH, Dijkman R, de Menezes RX, Commandeur S, Mulder AA, *et al*. Epigenetic profiling of cutaneous T-cell lymphoma: promoter hypermethylation of multiple tumor suppressor genes including BCL7a, PTPRG, and p73. J Clin Oncol. 2005;23(17):3886–96.
11. Lee JH, Khor TO, Shu L, Su Z-Y, Fuentes F, Kong A-NT. Dietary phytochemicals and cancer prevention: Nrf2 signaling, epigenetics, and cell death mechanisms in blocking cancer initiation and progression. Pharmacol Ther. 2013;137(2):153–71.
12. Su ZY, Zhang C, Lee JH, Shu L, Wu TY, Khor TO, et al. Requirement and epigenetics re-programming of Nrf2 in suppression of tumor promoter TPA-induced mouse skin cell transformation by sulforaphane. Cancer prevention research. 2014.
13. Su ZY, Shu L, Khor TO, Lee JH, Fuentes F, Kong AN. A perspective on dietary phytochemicals and cancer chemoprevention: oxidative stress, nrf2, and epigenomics. Top Curr Chem. 2013;329:133–62.
14. Yu S, Khor TO, Cheung K-L, Li W, Wu T-Y, Huang Y, *et al*. Nrf2 expression is regulated by epigenetic mechanisms in prostate cancer of TRAMP mice. PLoS One. 2010;5(1):e8579.
15. Hatzimichael E, Crook T. Cancer epigenetics: new therapies and new challenges. J Drug Deliv. 2013;2013:529312.
16. Katiyar SK, Singh T, Prasad R, Sun Q, Vaid M. Epigenetic alterations in ultraviolet radiation-induced skin carcinogenesis: interaction of bioactive dietary components on epigenetic targets. Photochem Photobiol. 2012;88(5):1066–74.
17. Baumann LS. Less-known botanical cosmeceuticals. Dermatol Ther. 2007;20(5):330–42.
18. Patel D, Shukla S, Gupta S. Apigenin and cancer chemoprevention: progress, potential and promise (review). Int J Oncol. 2007;30(1):233–45.
19. Shukla S, Gupta S. Apigenin: a promising molecule for cancer prevention. Pharm Res. 2010;27(6):962–78.
20. Merfort I, Heilmann J, Hagedorn-Leweke U, Lippold BC. In vivo skin penetration studies of camomile flavones. Pharmazie. 1994;49(7):509–11.
21. Li B, Birt DF. In vivo and in vitro percutaneous absorption of cancer preventive flavonoid apigenin in different vehicles in mouse skin. Pharm Res. 1996;13(11):1710–5.
22. Li B, Pinch H, Birt DF. Influence of vehicle, distant topical delivery, and biotransformation on the chemopreventive activity of apigenin, a plant flavonoid, in mouse skin. Pharm Res. 1996;13(10):1530–4.
23. Wei H, Tye L, Bresnick E, Birt DF. Inhibitory effect of apigenin, a plant flavonoid, on epidermal ornithine decarboxylase and skin tumor promotion in mice. Cancer Res. 1990;50(3):499–502.
24. Birt DF, Mitchell D, Gold B, Pour P, Pinch HC. Inhibition of ultraviolet light induced skin carcinogenesis in SKH-1 mice by apigenin, a plant flavonoid. Anticancer Res. 1997;17(1A):85–91.
25. Caltagirone S, Rossi C, Poggi A, Ranelletti FO, Natali PG, Brunetti M, *et al*. Flavonoids apigenin and quercetin inhibit melanoma growth and metastatic potential. Int J Cancer. 2000;87(4):595–600.
26. Fang M, Chen D, Yang CS. Dietary polyphenols may affect DNA methylation. J Nutr. 2007;137(1 Suppl):223S–8.
27. Pandey M, Kaur P, Shukla S, Abbas A, Fu P, Gupta S. Plant flavone apigenin inhibits HDAC and remodels chromatin to induce growth arrest and apoptosis in human prostate cancer cells: in vitro and in vivo study. Mol Carcinog. 2012;51(12):952–62.
28. Khor TO, Huang Y, Wu T-Y, Shu L, Lee J, Kong A-NT. Pharmacodynamics of curcumin as DNA hypomethylation agent in restoring the expression of Nrf2 via promoter CpGs demethylation. Biochem Pharmacol. 2011;82(9):1073–8.
29. Fuentes F, Shu L, Lee JH, Su Z-Y, Lee K-R, Kong A-NT. Nrf2-target approaches in cancer chemoprevention mediated by dietary phytochemicals. In: Bode AM, Dong Z, editors. Cancer prevention: methods in pharmacology and toxicology. New York: Springer; 2014. p. 53–83.
30. Ichihashi M, Ueda M, Budiyanto A, Bito T, Oka M, Fukunaga M, *et al*. UV-induced skin damage. Toxicology. 2003;189(1–2):21–39.
31. Schafer M, Dutsch S, auf dem Keller U, Werner S. Nrf2: a central regulator of UV protection in the epidermis. Cell Cycle. 2010;9(15):2917–8.
32. Xu C, Huang M-T, Shen G, Yuan X, Lin W, Khor TO, *et al*. Inhibition of 7,12-dimethylbenz(a)anthracene-induced skin tumorigenesis in C57BL/6 mice by sulforaphane is mediated by nuclear factor E2-related factor 2. Cancer Res. 2006;66(16):8293–6.
33. auf dem Keller U, Huber M, Beyer TA, Kumin A, Siemes C, Braun S, *et al*. Nrf transcription factors in keratinocytes are essential for skin tumor prevention but not for wound healing. Mol Cell Biol. 2006;26(10):3773–84.
34. Schafer M, Dutsch S, auf dem Keller U, Navid F, Schwarz A, Johnson DA. Nrf2 establishes a glutathione-mediated gradient of UVB cytoprotection in the epidermis. Genes Dev. 2010;24(10):1045–58.
35. Lepley DM, Pelling JC. Induction of p21/WAF1 and G1 cell-cycle arrest by the chemopreventive agent apigenin. Mol Carcinog. 1997;19(2):74–82.
36. McVean M, Weinberg WC, Pelling JC. A p21(waf1)-independent pathway for inhibitory phosphorylation of cyclin-dependent kinase p34(cdc2) and concomitant G(2)/M arrest by the chemopreventive flavonoid apigenin. Mol Carcinog. 2002;33(1):36–43.
37. Tong X, Pelling JC. Enhancement of p53 expression in keratinocytes by the bioflavonoid apigenin is associated with RNA-binding protein HuR. Mol Carcinog. 2009;48(2):118–29.
38. Huang YT, Kuo ML, Liu JY, Huang SY, Lin JK. Inhibitions of protein kinase C and proto-oncogene expressions in NIH 3 T3 cells by apigenin. Eur J Cancer. 1996;32A(1):146–51.
39. Tong X, Van Dross RT, Abu-Yousif A, Morrison AR, Pelling JC. Apigenin prevents UVB-induced cyclooxygenase 2 expression: coupled mRNA stabilization and translational inhibition. Mol Cell Biol. 2007;27(1):283–96.
40. Van Dross RT, Hong X, Pelling JC. Inhibition of TPA-induced cyclooxygenase-2 (COX-2) expression by apigenin through downregulation of Akt signal transduction in human keratinocytes. Mol Carcinog. 2005;44(2):83–91.
41. Byun S, Park J, Lee E, Lim S, Yu JG, Lee SJ, *et al*. Src kinase is a direct target of apigenin against UVB-induced skin inflammation. Carcinogenesis. 2013;34(2):397–405.
42. Arango D, Morohashi K, Yilmaz A, Kuramochi K, Parihar A, Brahimaj B, *et al*. Molecular basis for the action of a dietary flavonoid revealed by the comprehensive identification of apigenin human targets. Proc Natl Acad Sci U S A. 2013;110(24):E2153–62.
43. Lee WJ, Shim J-Y, Zhu BT. Mechanisms for the inhibition of DNA methyltransferases by tea catechins and bioflavonoids. Mol Pharmacol. 2005;68(4):1018–30.
44. Rajnee Kanwal HS, and Sanjay Gupta. Abstract 3683: Plant flavonoid apigenin preferentially binds with GC-rich DNA sequences and inhibits DNA methylation. AACR Proceedings of the 102nd Annual Meeting of the American Association for Cancer Research; Orlando, FL: Cancer Research April 15, 2011; Volume 71, Issue 8, Supplement 1; 2011.
45. Nguyen T, Kuo C, Nicholl MB, Sim MS, Turner RR, Morton DL, *et al*. Downregulation of microRNA-29c is associated with hypermethylation of tumor-related genes and disease outcome in cutaneous melanoma. Epigenetics: Off J DNA Methylation Soc. 2011;6(3):388–94.
46. Hadnagy A, Beaulieu R, Balicki D. Histone tail modifications and noncanonical functions of histones: perspectives in cancer epigenetics. Mol Cancer Ther. 2008;7(4):740–8.